Disclaimer

Autoantibodies to nodal isoforms of neurofascin in chronic inflammatory demyelinating polyneuropathy

Autoantibodies to nodal isoforms of neurofascin in chronic inflammatory demyelinating polyneuropathy

Emilien Delmont[1,2], Constance Manso[2], Luis Querol[3], Andrea Cortese[4], Angela Berardinelli[4], Alessandro Lozza[4], Maya Belghazi[1], Pauline Malissart[5], Pierre Labauge[5], Guillaume Taieb[5], Nobuhiro Yuki[6], Isabel Illa[3], Shahram Attarian[1], and Jérôme J. Devaux[2*]

[1]Referral Center for ALS and Neuromuscular Diseases, Timone University Hospital, AixMarseille University, France. [2]Aix-Marseille Université, CNRS, CRN2M-UMR7286, Marseille, France. [3]Neuromuscular Diseases Unit, Hospital de la Santa Creu i Sant Pau, Universitat Autónoma de Barcelona, Barcelona, Spain. [4]IRCCS, C. Mondino National Neurological Institute, Pavia, Italy. [5]Department of Neurology, Gui de Chauliac Hospital, Montpellier University Hospital Center, Montpellier, France. [6]Department of Neurology, Mishima Hospital, Niigata, Japan.

Running title: Autoantibodies to nodal Nfasc in CIDP

Corresponding authors: Jérôme J. Devaux, Ph.D.

Centre de Recherche en Neurobiologie et Neurophysiologie de Marseille - CRN2M, UMR 7286, CNRS, Aix-Marseille Université, Faculté de Médecine - Secteur Nord, CS80011, Bd Pierre Dramard, 13344 Marseille Cedex 15, France.

Phone: 33 491 69 89 44 Fax: 33 491 69 89 77 Email: jerome.devaux@univ-amu.fr

Author email addresses: EM, emilien.delmont@ap-hm.fr; CM, constance.manso@univamu.fr; LQ, LQuerol@santpau.cat; AC, andrea.cortese@mondino.it; AB, angela.berardinelli@mondino.it; AL, alessandro.lozza@mondino.it; MB, maya.belghazi@univamu.fr; PM, pauline.malissart@gmail.com; PL, p-labauge@chu-montpellier.fr; TG, gtaieb@chu-montpellier.fr; NY, gbs.yuki.cidp@gmail.com; II, IIlla@santpau.cat; SA, shahram.attarian@ap-hm.fr, JJD, jerome.devaux@univ-amu.fr

Title, 100 characters with spaces; running title, 37 characters with spaces; abstract, 317 words; manuscript, 5 056 words; figures, 5; tables, 3; supplemental figures, 4; supplemental tables, 2; references, 51.

Study funding: Supported by the Agence Nationale pour la Recherche (ACAMIN; JJD) under the frame of E-Rare-2, the ERA-Net for Research on Rare Diseases, the Association Française contre les Myopathies (MNM1 2012-14580; JJD, II, LQ), the JR14/00013 and I16/000627 grants from the Instituto de Salud Carlos III (LQ), and the PI13/00937 grant from the Instituto de Salud Carlos III (II). The mass spectrometer was obtained using financial support of the "Fédération de Recherche pour le Cerveau" (FRC) through the Rotary operation "Espoir en tête."

Financial disclosure statement: ED, CM, AC, AB, AL, MB, PM, PL, GT, NY, and SA have no relevant disclosures. JD received a research grant from CSL Behring. LQ received a travel grant from Bayer-Schering and research support from Fondo de Investigaciones Sanitarias, Subprograma Juan Rodes (JR14/00013). II received a travel grant from Genzyme, holds a patent for dysferlin detection in monocytes, has consulted for Grifols, and received research support from Fondo de Investigaciones Sanitarias, ISCIII, Ministry of Health (Spain), Fundacion Gemio.

Author contributions:

Drafting and revising of the manuscript, EM, CM, LQ, AC, AB, AL, MB, PM, PL, GT, NY, II, SA and JJD. Study concept and design, EM, LQ, AC, SA, and JD. Acquisition of data, EM, CM, LQ, AC, AB, AL, MB, PM, PL, GT, NY, II, SA, and JJD. Analysis and interpretation of data, EM, CM, LQ, AC, AB, AL, MB, PM, PL, GT, NY, II, SA and JJD.

Acknowledgments: We thank Romain Bernard and Axel Fernandez for technical assistance.

SUMMARY

Chronic inflammatory demyelination polyneuropathy is a heterogeneous and treatable immunemediated disorder that lacks biomarkers to support diagnosis. Recent evidences indicate that paranodal proteins (contactin-1, contactin-associated protein-1, and neurofascin-155) are the targets of autoantibodies in subsets of patients with chronic inflammatory demyelination polyneuropathy showing distinct clinical presentations. Particularly, these biomarkers appear to have clinical relevance and help orientate therapeutic choice. Here, we examined five patients presenting an IgG reactivity against the nodes of Ranvier and the axon initial segment. Using a proteomic approach, cell-based assays and ELISA, we identified neurofascin-186 (Nfasc186) and neurofascin-140 (Nfasc140) as the main targets of autoantibodies at the nodes of Ranvier.

Four patients displayed predominantly antibodies of the IgG4 subclass, whereas one patient presented IgG3 antibodies that activated the complement pathway *in vitro*. These antibodies recognized different epitopes than the previously described anti-neurofascin-155 IgG4 suggesting different pathogenic functions. Accordingly, patients with anti-Nfasc186/140 IgG showed a distinctive clinical presentation. Most patients had a severe phenotype associated with conduction block or decreased distal motor amplitude. Tremors or neuropathic pain were not observed. Four patients presented with a subacute-onset and sensory ataxia. In two patients, the neuropathy occurred concomitantly with nephrotic syndromes, or concomitantly with an IgG4related retroperitoneal fibrosis in another patient. This suggested that autoantibodies could be responsible for the occurrence of both disorders. Intravenous immunoglobulin and corticosteroids were effective in three patients, and one patient remitted following rituximab treatment. Clinical remission was found to correlate with the depletion of anti-Nfasc186/140 antibodies and the loss of IgG reactivity toward the nodes of Ranvier. In addition, recovery of conduction block and of distal motor amplitude were observed following remission and suggested a nodo-paranodopathy. Our data demonstrate that nodal antigens are the target of autoantibodies in a subgroup of patients with chronic inflammatory demyelination polyneuropathy. This emphasizes that the pathogenic mechanisms involved in chronic immunemediated demyelinating neuropathies are broad and may include dysfunctions of the nodes of Ranvier.

Keywords: paranode, myelin, CIDP, Guillain-Barré syndrome, IVIg

Abbreviations: Caspr1 = contactin-associated-protein-1, CIDP = chronic inflammatory demyelinating polyneuropathy, CNTN1 = contactin-1, FnIII = fibronectin type III, GBS = Guillain-Barré syndrome, HEK = human embryonic kidney, Ig = immunoglobulin, IVIg = intravenous immunoglobulin, Nav = voltage-gated sodium, Nfasc140 = neurofascin-140, Nfasc155 = neurofascin-155, Nfasc186 = neurofascin-186, PBS = phosphate buffered saline.

INTRODUCTION

Guillain-Barré syndrome (GBS) and chronic inflammatory demyelination polyneuropathy (CIDP) are rare and heterogeneous autoimmune diseases that affect peripheral nerves. Insofar, the pathogenic mechanisms responsible for these pathologies have been only partly unraveled (Yuki and Hartung, 2012; Mathey *et al.*, 2015; Goodfellow and Willison, 2016). Recent evidences indicate that the nodes of Ranvier can be the targets of the immune attack in GBS and in CIDP (Devaux *et al.*, 2012). Particularly, cell adhesion molecules at paranodes, contactin-1 (CNTN1), neurofascin-155 (Nfasc155), and contactin-associated protein 1 (Caspr1), have been shown to be selective targets of the IgG in subsets of CIDP patients (Ng *et al.*, 2012; Querol *et al.*, 2012; Querol *et al.*, 2014; Doppler *et al.*, 2015b; Miura *et al.*, 2015; Ogata *et al.*, 2015b; Devaux *et al.*, 2016; Doppler *et al.*, 2016). Patients with anti-Nfasc155 and CNTN1 IgG4 antibodies present with distinct clinical phenotypes including rapid severe onset, ataxia, tremor, and a poor response to intravenous immunoglobulin (IVIg) (Ng *et al.*, 2012; Querol *et al.*, 2012; Querol *et al.*, 2014; Miura *et al.*, 2015; Devaux *et al.*, 2016). By contrast, patients with anti-Caspr1 IgG showed neuropathic pain (Doppler *et al.*, 2016). The complex formed by the association of the glial Nfasc155 with the axonal CNTN1 and Caspr1 at paranodes is important for the formation and the maintenance of the voltage-gated sodium (Nav) channels at the nodes of Ranvier (Sherman *et al.*, 2005; Zonta *et al.*, 2008). Several evidences indicate that these antibodies are pathogenic as these affect the paranodal axo-glial junctions and induce conduction defects (Doppler *et al.*, 2015b; Doppler *et al.*, 2016; Manso *et al.*, 2016). The proportion of positive patients is still small (< 10%), but such antibodies can be helpful for patient prognosis and to guide treatments (Querol *et al.*, 2015).

Nodal antigens also seem to be targeted by autoantibodies in CIDP patients (Devaux *et al.*, 2012), however, the nature of these antigens is unclear insofar. In the peripheral nervous system, the Nav channels aggregation is dependent on the presence of cell adhesion molecule complexes at nodes and paranodes (Faivre-Sarrailh and Devaux, 2013). At nodal axolemma, neurofascin-186 (Nfasc186) interacts with gliomedin and NrCAM, two cell adhesion molecules secreted by Schwann cells, and enables the initial aggregation of the Nav channels at heminodes during development (Eshed *et al.*, 2005; Eshed *et al.*, 2007). Here, we examined a cohort of CIDP patients that showed IgG reaction against the nodes of Ranvier of murine sciatic nerve fibers. Using proteomic approaches, we identified neurofascin as the target of the autoantibodies in these patients. Our data indicate that patients' IgG react against Nfasc186 and neurofascin-140 (Nfasc140), the nodal isoforms of neurofascin. Interestingly, these patients present distinct

clinical features compared to those with anti-Nfasc155 IgG4. In some patients, the recovery of motor amplitudes following clinical remission was in keeping with the concept of nodo-paranodopathy (Uncini *et al.*, 2013). This data suggests the existence of chronic nodoparanodopathy where reversible conduction block coexists with demyelinating phenotypes.

METHODS

Patients and sera. Sera from 129 patients fulfilling the diagnostic criteria for CIDP (Joint Task Force of the EFNS and the PNS, 2010) were sent to the CRN2M from hospitals throughout France for anti-neurofascin antibody testing. Sera from CIDP patients from Spain, Italy, and Singapore were also sent for testing on teased murine sciatic nerve fibers. Clinical information from 5 CIDP patients that presented IgG reaction against the nodes of Ranvier and Nfasc140/186 was collected. As disease controls, we used sera from 26 patients with GBS, 32 with Charcot-Marie-Tooth disease, and 52 with multiple sclerosis. Besides, sera from 50 healthy controls were used. Written informed consent was obtained from each participant. The study was approved by the Ethics Committee of Aix-Marseille Université.

Constructs. Human Nfasc140 (XM_011509328.1) and Nfasc186 (NM_001005388.2) were amplified by PCR from a human brain cDNA library and sub-cloned into pcDNA3.1 (ThermoFisher scientific) at KpnI and EcoRI sites. Myc epitope was inserted at the intracellular C-terminal extremity using site-directed mutagenesis kit (Agilent technologies). All truncations were constructed from Myc-tagged human Nfasc140 using the site-directed mutagenesis kit.

Immunoprecipitation and mass spectrometry. For each immunoprecipitation, ten 100 mm plates of primary neocortical cell cultures were prepared from embryonic day 18 Wistar rats and were kept for 14 days *in vitro* as previously described (Miura *et al.*, 2015). Neurons were incubated for 1 hour at 37°C with CIDP or normal control sera diluted at 1:100 in neurobasal medium. After several washes, cells were solubilized in lysis buffer containing 1% Triton X100, 0.5% Na-deoxycholate, 150 mM NaCl, 100 mM Tris-HCl, pH 7.4 with protease inhibitors, then centrifuged at 18,900 x *g* for 30 minutes. The bound proteins were precipitated with a mixture of Protein A and G agarose beads (Sigma-Aldrich), released by boiling in SDS sample buffer for 2 minutes at 92°C, loaded on a 4-20% SDS-PAGE gel and stained with imperial blue (ThermoFisher scientific). Gel bands were rinsed with water and acetonitrile then reduced with DTT (Sigma-Aldrich), and alkylated with iodoacetamide (Sigma-Aldrich) and incubated overnight at 37°C in a microtube with 12.5 ng/µl of trypsin (Sequencing grade, Roche) in 25 mM NH_4HCO_3. The protein digests were sequenced by nano-LC–MS/MS (Dionex RSLC coupled to a hybrid Q orbitrap mass spectrometer equipped with a nano-ESI source; Q exactive ThermoFisher scientific) in the data-dependent acquisition mode (method top 10). Data were matched to the Uniprot protein database (Uniprot Swissprot, 548 454 sequences, version 2015 May, Taxonomy: Rattus, 7935 sequences) using the search engine Mascot version 2.2 (Matrix

Science, London, http://www.matrixscience.com) with the following search parameters: trypsin specificity, one missed cleavage, variable carbamidomethyl cysteine and oxidation of Met, and 10 ppm mass tolerance on precursor ion and 0.02 m/z on fragment ions.

Enzyme-linked immunosorbent assay (ELISA). Human recombinant Nfasc140 (15694H08H-50; Sino Biological Inc), Nfasc155 (8208-NF-050; R&D systems) and Nfasc186 (TP329070; OriGene Technologies) were diluted 1 µg/ml in phosphate-buffered saline (PBS). Microtiter plates were coated with 50 ng of recombinant protein overnight at 4°C. Wells were blocked for 1 hour at 37°C in blocking solution containing 0.5% casein sodium and 0.05% Tween-20 in PBS, then were incubated overnight at 4°C with the sera diluted in blocking buffer. Peroxidase-conjugated anti-human IgG (Jackson Immunoresearch) or peroxidase-conjugated anti-human IgG subclass-specific antibodies (IgG1, clone HP6069; IgG2, clone HP6014; IgG3, clone HP6047; and IgG4, clone HP6025; ThermoFisher Scientific) were added for 1 hour at 37°C. ELISA were developed with SIGMA*FAST* OPD tablets (Sigma-Aldrich), and optical densities were measured at 450 nm. All samples were tested in duplicate. To calculate antibody titers, sera were tested at serial dilutions (1:500–1:20,000). Sera were considered positive when the calculated optical density was higher than 3 standard deviations above the average healthy control signal at 1:500 dilution. For depletion experiments, sera diluted 1:500 were incubated overnight at 4°C on microtiter plate well coated with 50 ng of recombinant protein. The preincubated sera were then tested against Nfasc186 and Nfasc155 by ELISA as indicated above.

Complement binding assay. Microtiter plates were coated with 50 ng of Nfasc140 or Nfasc155, or with 100 ng of GM1 (Sigma-Aldrich). Wells were blocked and incubated overnight at 4°C with the sera diluted 1:20 in blocking buffer. Serum from a patient with acute motor axonal neuropathy with antibodies to GM1 was used as a positive control. Serum from a healthy control was used as a negative control. Serum dilution was adjusted to the antibody titer. The next day, the wells were incubated for 2 hours at room temperature with normal human sera as a source of complement diluted 1:10 in blocking buffer. Rabbit anti-human C1q antibodies (1:200; Abcam) was added for 1 hour at 37°C. Peroxidase-conjugated anti-rabbit IgG (1:2000; Jackson Immunoresearch) was finally added for 1 hour at 37°C, and ELISA were developed as described above.

Cell-binding assay and immunohistochemistry. Male C57BL/6J mice were euthanized and sciatic nerves were dissected out and fixed by immersion in 2% paraformaldehyde in PBS for 1 hour at 4°C, then rinsed in PBS. Fibers were gently teased and dried on glass slides, then kept

at -20°C. Teased fibers were permeabilized by immersion in -20°C acetone for 10 minutes, blocked at room temperature for 1 hour with 5% fish skin gelatin containing 0.1% Triton X100 in PBS and incubated overnight at 4°C with CIDP sera (1:200) and a goat antiserum against CNTN1 (1:2,000; R&D Systems). The slides were then washed several times and revealed with Alexa-conjugated secondary antibodies (1:500; Jackson ImmunoResearch).

Neocortical neurons were cultured on coverslips and kept 14 days *in vitro*, then were incubated with CIDP sera (1:200) in neurobasal medium (ThermoFisher Scientific) for 1 hour at 37°C, washed several times, and fixed with 2% paraformaldehyde for 20 minutes. Cells were permeabilized with PBS containing 5% fish skin gelatin and 0.1% Triton X-100, incubated for 1 hour at room temperature with rabbit antibodies against microtubule-associated protein 2 (MAP2; 1:500; EMD Millipore), and revealed with secondary antibodies.

Human embryonic kidney (HEK) cells were plated onto poly-L-lysine coated glass coverslips in 24-well plates at a density of 50,000 cells/wells and were transiently transfected using JetPEI (Polyplus-transfection). The day after, cells were incubated with serum free Opti-MEM medium (ThermoFisher Scientific) for 24 hours. Living cells were incubated for 20 min with sera diluted at 1:200 in Opti-MEM. After several washes, cells were fixed, permeabilized, incubated for 1 hour with a murine monoclonal antibodies against Myc (1:500; Roche), and for 30 minutes with secondary antibodies. Coverslips were then mounted.

Western-blot. HEK cells expressing Nfasc140, Nfasc155, or Nfasc186 were lysed for 15

minutes on ice in 1% Triton X-100, 140 mM NaCl, 20 mM Tris-HCl, pH 7.4 containing protease inhibitors, then centrifuged at 27,000 x *g* for 60 minutes. Proteins (50 µg) were denatured in SDS sample buffer for 2 minutes at 92°C, loaded on 7.5% SDS-PAGE gels, transferred, and immunoblotted with a CIDP sera (1:500) or the monoclonal antibodies against Myc (1:2000; Roche). Immunoreactivity was revealed using peroxidase-coupled donkey antimurine or anti-human secondary antibodies (1:5000; Jackson ImmunoResearch) and BM chemiluminescence kit (Sigma-Aldrich).

Statistics. Statistical significance was assessed by unpaired two-tailed Student's *t* tests or by one-way ANOVA followed by Bonferroni's post-hoc tests using GraphPad Prism (GraphPad Software). *P* values inferior to 0.05 were considered significant.

RESULTS

Case presentation

A 61-year-old man with no particular medical history had a sore throat and a bronchitis. One month after, he developed numbness of the four limbs and unsteadiness. Four months after the onset of the disease, examination revealed diffuse tendinous areflexia, socks and gloves hypoesthesia, sensory ataxia, proximal and distal muscle weaknesses and atrophy of the upper and lower limbs. Lumbar puncture revealed high proteinorachia (1.79 g/l) without cellular reaction. Initial nerve conduction study showed a sensory and motor demyelinating neuropathy (Supplemental Tables 1 and 2). Transcranial magnetic stimulation with triple stimulation technique showed a proximal conduction block on the left median nerve (Fig. 1). Antibodies against Ro/SSA antibodies were mildly positive. Anti-ganglioside antibodies, onconeural antibodies, blood electrophoresis, lip biopsy, bone marrow aspiration, all body scan and PET scan were normal. Sural nerve biopsy showed slight axonal loss (Fig. 1).

As the patient's condition did not improve despite IVIg and steroid therapies, plasma exchanges were assessed. The patient deteriorated dramatically the day after plasma exchange and was transferred to intensive care unit. He was bedridden, with cranial nerves involvement (V, VII, IX and oculomotor nerves) and needed mechanical ventilation for a week. Blink reflex showed at this time bilateral increased latency of R1 reflex. IVIg infusions were then repeated and elicited muscle strength improvement but the efficacy lasted only few days and infusions had to be done every 2 weeks then every one week despite three cyclophosphamide infusions. Rituximab (4 weekly 375 mg/m^2 infusions) was administrated at this time and progressively the patient recovered and IVIg withdrawal was possible. After 1 year of follow-up, neurological examination, nerve conduction studies and transcranial magnetic stimulation with triple stimulation technique were normal (Supplemental Tables 1 and 2). After 2 years of follow-up, the patient takes no treatment and has no neurological complains.

The presence of conduction block, prompt worsening and improvement of motor amplitudes after therapy were suggestive of a nodo-paranodopathy. The patient serum was thus tested for the presence of antibodies against nodal or paranodal proteins.

Identification of neurofascin as a target for autoantibodies at the nodes of Ranvier

The serum sample was first tested on teased nerve fibers to screen for reactivity against nodes, paranodes, or myelin compartments. Patient's IgG strongly reacted toward the nodes of Ranvier (Fig. 2). Because many components found at the nodes are also expressed in the axon initial segment of neurons, the serum was also tested on live neocortical neurons in culture in order to identify the target antigens. Patient's IgG bound to surface epitopes located on the axon initial

segments identified using ankyrin-G (Fig. 2). The patient's serum and the serum from a healthy control were then used for immunoprecipitation. Two protein bands were identified with the CIDP patient serum around 100-140 kDa and 150-190 kDa (Fig. 2C). Both bands were identified as neurofascin by mass spectrometry, and the peptide identified by mass spectrometry matched with all isoforms of neurofascin (Fig. 2D and Supplemental Fig. 1). Three main isoforms of neurofascin have been described in the peripheral nervous system: Nfasc140, Nfasc155, and Nfasc186 (Basak *et al.*, 2007; Zhang *et al.*, 2015). Nfasc155 is expressed by glial cells and located at paranodes (Tait *et al.*, 2000; Charles *et al.*, 2002). By contrast, Nfasc140 and Nfasc186 are neuronal and found at nodes of Ranvier and axon initial segments (Davis *et al.*, 1996; Zhang *et al.*, 2015). The fact that the IgG immunoprecipitated two protein bands from axon initial segments and that patient's IgG reacted only against the node of Ranvier suggested that it reacted against Nfasc140 and Nfasc186.

To validate this hypothesis, we cloned human Nfasc140 and Nfasc186, and inserted these constructs in mammalian expression vector with a Myc epitope attached to the intracellular Cterminal end. We then tested the patient's serum on HEK cells transiently expressing either Nfasc140, Nfasc155, or Nfasc186 (Fig. 3). The IgG strongly reacted against Nfasc140 and Nfasc186, and much less to Nfasc155. As controls, we tested sera from healthy controls. No healthy controls reacted against Nfasc140, Nfasc155, or Nfasc186 (Fig. 3). These results clearly indicated that the patient's IgG reacted against nodal isoforms of neurofascin, however, the antibodies also seemed to react against Nfasc155. In a previous study, we showed that CIDP patients presenting with anti-Nfasc155 IgG4 do not react with Nfasc186 and do not bind neurons in cultures (Devaux *et al.*, 2016). This observation was confirmed here.

The serum IgG from five French CIDP patients with anti-Nfasc155 IgG4 were tested against neurons and transfected HEK cells, and did not show reactivity against axon initial segments (Supplemental Fig. 2) or Nfasc140 or Nfasc186 (Supplemental Fig. 3C). This indicated that the different CIDP patients presented autoantibodies targeting distinct epitopes. Anti-Nfasc155 IgG4 binds specific epitopes on Nfasc155 at paranodes. By contrast, antibodies from patient CIDP1 target epitopes common to all neurofascin isoforms and predominantly target the nodes. It is worth noting that monoclonal antibodies reacting against the cytosolic region of all neurofascin isoforms also predominantly stain the nodal region (Lonigro and Devaux, 2009). The predominant fixation of autoantibodies from patient CIDP1 at nodes may thus be reflective of the higher amount of Nfasc186 at nodes. For clarity, we propose to call these latter antiNfasc140/186 IgG, as these target predominantly the nodes of Ranvier.

Epitope and isotype identification of anti-Nfasc140/186 autoantibodies

To characterize the prevalence and specificity of anti-Nfasc140/186 antibodies, but also IgG titers and isotypes, cohorts of French CIDP (n = 129), GBS (n = 26), Charcot-Marie-Tooth (n = 32), and multiple sclerosis patients (n = 52) were screened by ELISA against Nfasc140, Nfasc155, or Nfasc186. Sera from 50 healthy donors were used as controls. Anti-Nfasc140/186 IgG were identified in sera from 2 French CIDP patients (2%), but not in those from patients with GBS, Charcot-Marie-Tooth and multiple sclerosis patients or from healthy controls. IgG from patient CIDP1 reacted toward Nfasc140, Nfasc155 and Nfasc186 by ELISA (Table 1), whereas those from patient CIDP2 reacted against Nfasc186 only. Similar finding were observed on transfected cells. IgG from patient CIDP2 only marginally reacted against Nfasc140 or Nfasc155 at a 1:50 dilution (Supplemental Fig. 3), indicating that autoantibodies reacted against a specific region of Nfasc186, and only marginally recognized the other isoforms. Of interest, the antibodies of both patients were predominantly of the IgG4 subclass. As mentioned above, anti-Nfasc155 IgG4 autoantibodies were detected in five French CIDP patients (4%). These did not react to Nfasc140 or Nfasc186 by ELISA (Table 1) or cell based assays (Supplemental Fig. 3).

During the last years, several serum samples of CIDP patients from centers in Spain, Italy, and Singapore were sent to us for testing on teased nerve fibers and neuronal cultures. Of interest, several samples reacted against nodes of Ranvier and the axon initial segments, in a similar manner as the French CIDP patients (Supplemental Fig. 2). To determine whether neurofascin could be the target antigens, we tested these samples by ELISA and cell based assays. We identified three patients reacting against Nfasc140, Nfasc155, and Nfasc186 using both ELISA and cell based assays (Table 1 and Supplemental Fig. 3). These three patients presented a relatively similar reactivity toward the three neurofascin isoforms. The IgG subclass was predominantly IgG4 in two patients, and IgG3 in one patient (Table 1). The reactivity to neurofascin isoforms, the isotype determination, and the reactivity against the nodes of Ranvier were tested independently in two centers (CRN2M and Neuromuscular Diseases Unit), and gave consistent results.

To determine whether anti-Nfasc140/186 IgG recognizes a common region in Nfasc140, Nfasc155, or Nfasc186, the positive sera were pre-incubated with the neurofascin isoforms *in vitro*, this in order to deplete the antibodies reacting against these isoforms. Then, the depleted sera were tested against Nfac155 or Nfasc186 by ELISA, and compared to the reactivity of the

non-depleted sera (Fig. 4A). Pre-incubation of sera from patients CIDP1 to 5 with any neurofascin isoforms significantly decreased the ELISA signal against Nfasc155 or Nfasc186, while pre-incubation of serum CIDP6 with Nfasc140 or Nfasc186 did not alter ELISA signal against Nfasc155. This indicated that anti-Nfasc140/186 IgG recognizes a common epitope that is comprised within the peptide sequence of Nfasc140. Neurofascin isoforms are composed of six immunoglobulin (Ig) domains, and three to four fibronectin type III (FnIII) domains (Fig. 2). Nfasc155 only differs from Nfasc140 by the presence of a fourth FnIII domain. Because anti-Nfasc155 IgG4 did not react against Nfasc140 (Fig. 4, Table 1 and Supplemental Fig. 3), it clearly appears that the antibodies specifically target the FnIII domain exclusive to Nfasc155. To determine the domains that are targeted by anti-Nfasc140/186 IgG within the sequence of Nfasc140, we deleted the Ig or FnIII domains of Nfasc140 and tested serum reactivity against these constructs in HEK cells. All the sera reacted against the Ig domains of Nfasc140 that are common to all neurofascin isoforms (Fig. 4D). By contrast, the samples did not react against the FnIII domains of Nfasc140 (Fig. 4C). This further indicated that anti-Nfasc140/186 IgG targets epitopes different from those recognized by anti-Nfasc155 IgG4.

IgG4 is known to weakly activate the complement pathway (Huijbers *et al.*, 2015). Here, one patient showed a predominant IgG3 response, and some presented a weak IgG2 response. We thus suspected that these antibodies may effect, even partially, through the complement pathway. To determine this, antibody potency to fix C1q was tested *in vitro*. As positive control, the serum from a patient with acute motor axonal neuropathy presenting IgG against GM1 was used. As expected, the anti-GM1 IgG from this patient strongly fixed C1q *in vitro* (Fig. 4E) compared to serum from a healthy control. None of the patients with anti-Nfasc155 IgG4 fixed C1q. Only one patient with anti-Nfasc140/186 IgG fixed complement *in vitro*. This activity matched with the predominant IgG3 response in this patient.

Clinical features of anti-Nfasc140/186 IgG-positive CIDP patients

Clinical data were available for the five patients (Tables 2 and 3, and Supplemental Tables 1 and 2). The clinical history of the pediatric case is detailed in Appendix 1. All patients had a symmetric sensory and motor polyradiculoneuropathy. The neuropathy was severe at disease nadir: all patients were unable to walk without aid, and two patients had cranial nerve impairments and needed a transient mechanical ventilation in an intensive care unit. On the opposite, after therapy, all the patients were able to walk without aid at the last follow-up. Three patients improved after IVIg, and immunosuppressive drugs appeared to be effective in one of

these patients. Three patients also improved after steroids. It is noticeable that four patients presented with a concomitant autoimmune disorders: one patient had a retroperitoneal fibrosis, one had anti-Ro/SSA antibodies, and two presented with nephrotic syndromes concomitant to the neuropathy. Biopsies indicated that one patient presented membranous nephropathy and the other focal segmental glomerulosclerosis (Quek *et al.*, 2014). No patients presented evidence of tumors withstanding a paraneoplastic origin.

Nerve conduction studies revealed a demyelinating neuropathy with conduction blocks in three patients and an axonal neuropathy in the two remaining patients. CSF analysis showed high protein levels (median 1.79g/l, range 0.8-2g/l). Patients with Nfasc140/186 IgG antibodies were compared to 74 previously reported patients with anti-Nfasc155 IgG4 antibodies (Ng *et al.*, 2012; Querol *et al.*, 2014; Ogata *et al.*, 2015b; Devaux *et al.*, 2016; Kadoya *et al.*, 2016) and 76 CIDP patients without antibodies against neurofascin isoforms fulfilling the EFNS/PNS CIDP diagnostic criteria (Joint Task Force of the EFNS and the PNS, 2010) followed in the neuromuscular referral center of Marseille (Table 3). Patients with Nfasc140/186 IgG antibodies presented more frequently with a subacute-onset, did not demonstrate tremors and seemed more responsive to IVIg than patients with anti-Nfasc155 IgG4. Patients with Nfasc140/186 IgG antibodies also presented a more severe phenotype than seronegative CIDP patients.

Antibody titers after clinical recovery

Serum samples from two CIDP patients (CIDP1 and 4) were available after clinical recovery. Titration of anti-Nfasc140/186 antibodies by ELISA indicated a complete depletion of the antibodies in both patients that correlated with the clinical improvements at one and two years after onset for CIDP1 and at 3 and 6 months after onset for CIDP4 (Fig. 5). In addition, serum IgG binding to nodes of Ranvier, axon initial segments, and transfected HEK cells was completely abolished (Supplemental Fig. 4). This further confirmed that the reactivity toward nodes of Ranvier is specifically related to the presence of anti-Nfasc140/186 antibodies.

DISCUSSION

We here identified using immunoprecipitation autoantibodies against Nfasc140 and Nfasc186, two nodal isoforms of neurofascin, in a CIDP patient. This patient showed proximal conduction

block, a rapid deterioration, improvement after therapy, and a recovery of motor amplitudes on nerve conduction studies that matched with the concept of nodo-paranodopathy. Further, we demonstrated that anti-Nfasc140/186 IgG are associated with a subset of CIDP patients. These antibodies were mostly IgG4 and differed from the previously described anti-Nfasc155 IgG4. Antibodies to Nfasc155 recognized specifically the third FnIII domain that is exclusive to Nfasc155 and bound to the paranodes. By contrast, anti-Nfasc140/186 IgG reacted against the Ig domains that are common to all neurofascin isoforms, and bound more prominently to the nodes of Ranvier. In addition, the clinical features of the CIDP patients with anti-Nfasc140/186 IgG differ from those with anti-Nfasc155 IgG4, but also from seronegative CIDP patients, indicating that these patients form a distinct subgroup.

We found that anti-Nfasc140/186 IgG are associated with a subset of CIDP patients showing subacute-onset (4/5), sensory ataxia (4/5), conduction block (3/5), and cranial nerve involvement (2/5). Previous studies have also examined the prevalence of antibodies to Nfasc155 and Nfasc186 in CIDP and multifocal motor neuropathy but concluded that patients lack reactivity to Nfasc186 (Ng *et al.*, 2012; Ogata *et al.*, 2015a; Devaux *et al.*, 2016; Doppler *et al.*, 2015a). This discrepancy may be due to the low prevalence of these autoantibodies. Here, these antibodies were detected in only 2% of CIDP patients. In addition, we also reported antibodies to Nfasc186 in a small percentage of Japanese CIDP and GBS patients (Devaux et al., 2012). Most patients with anti-Nfasc140/186 IgG were responsive to IVIg treatments and showed a good response to steroids. No patients showed tremors or neuropathic pain. This contrasted with patients seropositive for anti-Nfasc155, CNTN1 or Caspr1 IgG4 (Ng *et al.*, 2012; Querol *et al.*, 2012; Querol *et al.*, 2014; Doppler *et al.*, 2015b; Miura *et al.*, 2015; Ogata *et al.*, 2015b; Devaux *et al.*, 2016; Doppler *et al.*, 2016). Of interest, four patients (4/5) presented with a concomitant autoimmune disorder. Two patients presented with a nephrotic syndrome, one with retroperitoneal fibrosis, and one presented anti-Ro/SSA antibodies. This association suggest that either anti-Nfasc140/186 IgG are responsible for the occurrence of both disorders, or that one disorder is secondary to the other. The fact that the autoimmune diseases occurred concomitantly is in favor of the first hypothesis. Concerning the nephrotic syndrome, neurofascin was shown to be expressed in human kidney glomeruli (Sistani *et al.*, 2013). It is thus plausible that anti-Nfasc140/186 IgG are responsible for both disorders. The occurrence of GBS or CIDP and nephrotic syndrome is not common but several cases have been reported in the literature (Kohli *et al.*, 1992; Wu *et al.*, 2001; Chen *et al.*, 2006; Smyth and Menkes, 2008; Souayah *et al.*, 2008; Filippone *et al.*, 2013). Insofar, the link between these two disorders has

been a matter of discussion. Our data indicate that anti-Nfasc140/186 IgG should be investigated in these cases. Biopsies of the retroperitoneal fibrosis further revealed the presence of IgG4-positive plasma cells. Albeit, the presence of neurofascin in the retroperitoneal mass is unknown, this suggests that these autoimmune disorders are mediated by IgG4 autoantibodies and involve common pathogenic mechanisms.

The depletion of anti-Nfasc140/186 IgG correlated with clinical remission in two patients further indicating that autoantibodies may be responsible for the pathology. In both patients, nerve conduction study findings were in part consistent with the concept of nodoparanodopathy (Uncini *et al.*, 2013). One patient showed recovery of a proximal conduction block after treatment, whereas the other presented a recovery of distal amplitudes, suggesting a reversible conduction failure. Nonetheless, all patients fulfilled the criteria for CIDP, and were negative for anti-gangliosides antibodies. These results indicate that anti-Nfasc140/186 IgG may induce dysfunctions at the nodes of Ranvier and a chronic nodo-paranodopathy characterized by reversible conduction block coexisting with demyelinating features. These latter findings challenge the original concept of nodo-paranodopathy, and show that autoantibodies against nodal components do not necessarily induce conduction block and an axonal-like pathology. The mechanisms how these antibodies mediate conduction deficits have yet to be identified. In most patients, antibodies were predominantly of the IgG4 isotype and did not fix C1q *in vitro*. This was in keeping with the fact that IgG4 antibodies do not activate the classical complement pathway (Huijbers *et al.*, 2015) and argued against a complement attack at nodes. In contrast to patients with anti-Nfasc155 IgG4, IVIg treatments induced clear clinical improvements in these patients. Only one patient showed a predominant IgG3 reactivity against Nfasc186 and Nfasc140. These antibodies activated complement *in vitro*, but the patient did not respond to IVIg.

Our hypothesis is that IgG4 autoantibodies affect specifically the nodal physiology. Several evidences indicate that IgG4 against CNTN1 or Nfasc155 disrupt paranode organization. Loss of paranodal axo-glial complexes was observed in skin biopsies of patients with anti-CNTN1 IgG4 (Doppler *et al.*, 2015b) and after passive transfer of anti-CNTN1 IgG4 in animal models (Manso *et al.*, 2016). Anti-CNTN1 IgG4 has also been shown to disrupt the interaction between CNTN1/Caspr1 and Nfasc155 *in vitro* (Labasque *et al.*, 2014), and to penetrate the paranodal regions (Manso *et al.*, 2016). Moreover, paranodes lack septate-like junctions in sural nerve biopsies from patients with anti-Nfasc155 IgG4 (Vallat *et al.*, 2016). In myasthenia gravis, antimuscle-specific kinase IgG4 were also shown to block the interaction between muscle-

specific kinase and low-density lipoprotein receptor-related protein 4 (Huijbers *et al.*, 2013). It thus plausible that anti-Nfasc140/186 IgG also affects the axo-glial interaction at nodes and leads to conduction loss or slowing. In keeping, anti-Nfasc140/186 IgG targeted predominantly the Ig domains of neurofascin that are known to play a role in both homo- and heterophilic interactions (Faivre-Sarrailh and Devaux, 2013). Deletion of Nfasc186 Ig domains abolishes its accumulation at the nodes (Dzhashiashvili *et al.*, 2007) and the deletion of neurofascin abolishes Nav channel aggregation at the nodes (Sherman *et al.*, 2005). In a previous study, we found that anti-gliomedin antibodies induce nodal elongation and the loss of Nav channel aggregates at nodes in animal models (Devaux, 2012). Anti-Nfasc186 IgG were also found to exacerbate the clinical signs of experimental allergic encephalitis and neuritis and to induce axonal injury in the CNS (Mathey *et al.*, 2007; Lindner *et al.*, 2013; Yan *et al.*, 2014). This indicates that, in animal models, these antibodies can be pathogenic. In a similar manner as anti-GM1 antibodies (Susuki *et al.*, 2007; Susuki *et al.*, 2012), we suspect that antiNfasc140/186 IgG can induce functional alterations at the nodes that can be promptly alleviated by treatments. In addition, these antibodies may induce more dramatic deteriorations leading to demyelination and axonal loss. The importance of the reactivity toward Nfasc140 is unclear as this isoform is predominantly expressed at early developmental stages (Zhang *et al.*, 2015). Nonetheless, the transgenic expression of Nfasc140 in neurofascin null mice indicates that this isoform is also expressed at nodes at adult ages. Nfasc140 expression is also strongly increased in demyelinated white matter regions of multiple sclerosis patients (Zhang *et al.*, 2015). The reexpression of Nfasc140 after demyelination may thus favor autoantibodies attack and disease progression.

An intriguing point is the difference in IVIg response of patients with anti-Nfasc155 IgG4 or anti-Nfasc140/186 IgG. Because both autoantibodies do not activate complement *in vitro*, it suggests that IVIg response depends on other factors than solely the complement pathway. IVIg is known to act through multiple pathways (Schwab and Nimmerjahn, 2013). One possibility could be that anti-idiotypic antibodies present in IVIg transiently scavenge anti-Nfasc140/186 IgG. Another possibility could be that anti-Nfasc140/186 IgG induces functional alterations at nodes that are more easily alleviated by IVIg than disruptions of the paranodal septate-like junctions induced by anti-Nfasc155 IgG4.

In conclusion, our data indicate that nodal neurofascin isoforms are additional autoantibodies targets in CIDP patients, and that these biomarkers can be useful for treatment choice. These patients show different clinical features than those previously described, and further pinpoint

that CIDP is a heterogeneous autoimmune disorder with multiple immune targets and pathogenic mechanisms.

REFERENCES

Basak S, Raju K, Babiarz J, Kane-Goldsmith N, Koticha D, Grumet M. Differential expression and functions of neuronal and glial neurofascin isoforms and splice variants during PNS development. Dev Biol 2007; 311(2): 408-22.

Charles P, Tait S, Faivre-Sarrailh C, Barbin G, Gunn-Moore F, Denisenko-Nehrbass N*, et al.* Neurofascin is a glial receptor for the paranodin/Caspr-contactin axonal complex at the axoglial junction. Curr Biol 2002; 12(3): 217-20.

Chen KH, Chang CT, Hung CC. Glomerulonephritis associated with chronic inflammatory demyelinating polyneuropathy. Ren Fail 2006; 28(3): 255-9.

Davis JQ, Lambert S, Bennett V. Molecular composition of the node of Ranvier: identification of ankyrin-binding cell adhesion molecules neurofascin (mucin+ third FNIII domain-) and NrCAM at nodal axon segments. J Cell Biol 1996; 135(5): 1355-67.

Devaux JJ. Antibodies to gliomedin cause peripheral demyelinating neuropathy and the dismantling of the nodes of ranvier. Am J Pathol 2012; 181(4): 1402-13.

Devaux JJ, Miura Y, Fukami Y, Inoue T, Manso C, Belghazi M*, et al.* Neurofascin-155 IgG4 in chronic inflammatory demyelinating polyneuropathy. Neurology 2016; 86(9): 800-7.

Devaux JJ, Odaka M, Yuki N. Nodal proteins are target antigens in Guillain-Barré syndrome. J Peripher Nerv Syst 2012; 17(1): 62-71.

Doppler K, Appeltshauser L, Kramer HH, Ng JK, Meinl E, Villmann C*, et al.* Contactin-1 and Neurofascin-155/-186 are not targets of auto-antibodies in multifocal motor neuropathy. PLoS One 2015a; 10(7): e0134274.

Doppler K, Appeltshauser L, Villmann C, Martin C, Peles E, Kramer HH*, et al.* Auto-antibodies to contactin-associated protein 1 (Caspr) in two patients with painful inflammatory neuropathy. Brain 2016; 139(Pt 10):2617-2630.

Doppler K, Appeltshauser L, Wilhelmi K, Villmann C, Dib-Hajj SD, Waxman SG*, et al.* Destruction of paranodal architecture in inflammatory neuropathy with anti-contactin-1 autoantibodies. J Neurol Neurosurg Psychiatry 2015b; 86(7):720-8.

Dzhashiashvili Y, Zhang Y, Galinska J, Lam I, Grumet M, Salzer JL. Nodes of Ranvier and axon initial segments are ankyrin G-dependent domains that assemble by distinct mechanisms. J Cell Biol 2007; 177(5): 857-70.

Eshed Y, Feinberg K, Carey DJ, Peles E. Secreted gliomedin is a perinodal matrix component of peripheral nerves. J Cell Biol 2007; 177(3): 551-62.

Eshed Y, Feinberg K, Poliak S, Sabanay H, SarigNadir O, Spiegel I*, et al.* Gliomedin mediates Schwann cell-axon interaction and the molecular assembly of the nodes of Ranvier. Neuron 2005; 47(2): 215-29.

Faivre-Sarrailh C, Devaux JJ. Neuro-glial interactions at the nodes of Ranvier: implication in health and diseases. Front Cell Neurosci 2013; 7: 196.

Filippone EJ, Kanzaria M, Bell R, Newman E, J LF. Secondary membranous nephropathy associated with Guillain-Barré syndrome. Case Rep Nephrol Urol 2013; 3(1): 34-9.

Goodfellow JA, Willison HJ. Guillain-Barré syndrome: a century of progress. Nat Rev Neurol 2016; 12(12): 723-31.

Huijbers MG, Querol LA, Niks EH, Plomp JJ, van der Maarel SM, Graus F*, et al.* The expanding field of IgG4-mediated neurological autoimmune disorders. Eur J Neurol 2015; 22(8): 1151-61.

Huijbers MG, Zhang W, Klooster R, Niks EH, Friese MB, Straasheijm KR*, et al.* MuSK IgG4 autoantibodies cause myasthenia gravis by inhibiting binding between MuSK and Lrp4. Proc Natl Acad Sci U S A 2013; 110(51): 20783-8.

Joint Task Force of the EFNS and the PNS. European Federation of Neurological Societies/Peripheral Nerve Society Guideline on management of chronic inflammatory demyelinating polyradiculoneuropathy: report of a joint task force of the European Federation of Neurological Societies and the Peripheral Nerve Society - First Revision. J Peripher Nerv Syst 2010; 15(4): 373.

Kadoya M, Kaida K, Koike H, Takazaki H, Ogata H, Moriguchi K*, et al.* IgG4 antineurofascin155 antibodies in chronic inflammatory demyelinating polyradiculoneuropathy: clinical significance and diagnostic utility of a conventional assay. J Neuroimmunol 2016; 301: 16-22.

Kohli A, Tandon P, Kher V. Chronic inflammatory demyelinating polyradiculoneuropathy with membranous glomerulonephritis: report of one case. Clin Neurol Neurosurg 1992; 94(1): 31-3.

Labasque M, Hivert B, Nogales-Gadea G, Querol L, Illa I, Faivre-Sarrailh C. Specific contactin *N*-glycans are implicated in neurofascin binding and autoimmune targeting in peripheral neuropathies. J Biol Chem 2014; 289(11): 7907-18.

Lindner M, Ng JK, Hochmeister S, Meinl E, Linington C. Neurofascin 186 specific autoantibodies induce axonal injury and exacerbate disease severity in experimental autoimmune encephalomyelitis. Exp Neurol 2013; 247: 259-66.

Lonigro A, Devaux JJ. Disruption of neurofascin and gliomedin at nodes of Ranvier precedes demyelination in experimental allergic neuritis. Brain 2009; 132(Pt 1): 260-73.

Manso C, Querol L, Mekaouche M, Illa I, Devaux JJ. Contactin-1 IgG4 antibodies cause paranode dismantling and conduction defects. Brain 2016; 139(Pt 6): 1700-12.

Mathey EK, Derfuss T, Storch MK, Williams KR, Hales K, Woolley DR*, et al.* Neurofascin as a novel target for autoantibody-mediated axonal injury. J Exp Med 2007; 204(10): 2363-72.

Mathey EK, Park SB, Hughes RA, Pollard JD, Armati PJ, Barnett MH*, et al.* Chronic inflammatory demyelinating polyradiculoneuropathy: from pathology to phenotype. J Neurol Neurosurg Psychiatry 2015; 86(9): 973-85.

Miura Y, Devaux JJ, Fukami Y, Manso C, Belghazi M, Wong AH*, et al.* Contactin 1 IgG4 associates to chronic inflammatory demyelinating polyneuropathy with sensory ataxia. Brain 2015; 138(Pt 6): 1484-91.

Ng JK, Malotka J, Kawakami N, Derfuss T, Khademi M, Olsson T*, et al.* Neurofascin as a target for autoantibodies in peripheral neuropathies. Neurology 2012; 79(23): 2241-8.

Ogata H, Matsuse D, Yamasaki R, Kawamura N, Matsushita T, Yonekawa T*, et al.* A nationwide survey of combined central and peripheral demyelination in Japan. J Neurol Neurosurg Psychiatry 2015a; 87(1):29-36.

Ogata H, Yamasaki R, Hiwatashi A, Oka N, Kawamura N, Matsuse D*, et al.* Characterization of IgG4 anti-neurofascin 155 antibody-positive polyneuropathy. Ann Clin Transl Neurol 2015b; 2(10): 960-71.

Quek AM, Soon D, Chan YC, Thamboo TP, Yuki N. Acute-onset chronic inflammatory demyelinating polyneuropathy with focal segmental glomerulosclerosis. J Neurol Sci 2014; 341(1-2): 139-43.

Querol L, Nogales-Gadea G, Rojas-Garcia R, Diaz-Manera J, Pardo J, Ortega-Moreno A*, et al.* Neurofascin IgG4 antibodies in CIDP associate with disabling tremor and poor response to IVIg. Neurology 2014; 82(10): 879-86.

Querol L, Nogales-Gadea G, Rojas-Garcia R, Martinez-Hernandez E, Diaz-Manera J, SuarezCalvet X*, et al.* Antibodies to contactin-1 in chronic inflammatory demyelinating polyneuropathy. Ann Neurol 2012; 73(3): 370-80.

Querol L, Rojas-Garcia R, Diaz-Manera J, Barcena J, Pardo J, Ortega-Moreno A*, et al.* Rituximab in treatment-resistant CIDP with antibodies against paranodal proteins. Neurol Neuroimmunol Neuroinflamm 2015; 2(5): e149.

Schwab I, Nimmerjahn F. Intravenous immunoglobulin therapy: how does IgG modulate the immune system? Nat Rev Immunol 2013; 13(3): 176-89.

Sherman DL, Tait S, Melrose S, Johnson R, Zonta B, Court FA*, et al.* Neurofascins are required to establish axonal domains for saltatory conduction. Neuron 2005; 48(5): 737-42.

Sistani L, Rodriguez PQ, Hultenby K, Uhlen M, Betsholtz C, Jalanko H*, et al.* Neuronal proteins are novel components of podocyte major processes and their expression in glomerular crescents supports their role in crescent formation. Kidney Int 2013; 83(1): 63-71.

Smyth S, Menkes DL. Coincident membranous glomerulonephritis and chronic inflammatory demyelinating polyradiculoneuropathy: questioning the autoimmunity hypothesis. Muscle Nerve 2008; 37(1): 130-5.

Souayah N, Cros D, Stein TD, Chong PS. Relapsing Guillain-Barré syndrome and nephrotic syndrome secondary to focal segmental glomerulosclerosis. J Neurol Sci 2008; 270(1-2): 184-8.

Susuki K, Rasband MN, Tohyama K, Koibuchi K, Okamoto S, Funakoshi K*, et al.* Anti-GM1 antibodies cause complement-mediated disruption of sodium channel clusters in peripheral motor nerve fibers. J Neurosci 2007; 27(15): 3956-67.

Susuki K, Yuki N, Schafer DP, Hirata K, Zhang G, Funakoshi K*, et al.* Dysfunction of nodes of Ranvier: a mechanism for anti-ganglioside antibody-mediated neuropathies. Exp Neurol 2012; 233(1): 534-42.

Tait S, Gunn-Moore F, Collinson JM, Huang J, Lubetzki C, Pedraza L*, et al.* An oligodendrocyte cell adhesion molecule at the site of assembly of the paranodal axo-glial junction. J Cell Biol 2000; 150(3): 657-66.

Uncini A, Susuki K, Yuki N. Nodo-paranodopathy: beyond the demyelinating and axonal classification in anti-ganglioside antibody-mediated neuropathies. Clin Neurophysiol 2013; 124(10):1928-34.

Vallat JM, Yuki N, Sekiguchi K, Kokubun N, Oka N, Mathis S*, et al.* Paranodal lesions in chronic inflammatory demyelinating polyneuropathy associated with anti-Neurofascin 155 antibodies. Neuromuscul Disord 2016; doi: 10.1016/j.nmd.2016.10.008.

Wu AD, Russell JA, Bouthout BA. Chronic inflammatory demyelinating polyneuropathy and membranous glomerulonephropathy: report of two cases. J Clin Neuromuscul Dis 2001; 3(2): 70-4.

Yan W, Nguyen T, Yuki N, Ji Q, Yiannikas C, Pollard JD*, et al.* Antibodies to neurofascin exacerbate adoptive transfer experimental autoimmune neuritis. J Neuroimmunol 2014; 277(1-2): 13-7.

Yuki N, Hartung HP. Guillain-Barré syndrome. N Engl J Med 2012; 366(24): 2294-304.

Zhang A, Desmazieres A, Zonta B, Melrose S, Campbell G, Mahad D*, et al.* Neurofascin 140 is an embryonic neuronal neurofascin isoform that promotes the assembly of the node of Ranvier. J Neurosci 2015; 35(5): 2246-54.

Zonta B, Tait S, Melrose S, Anderson H, Harroch S, Higginson J*, et al.* Glial and neuronal isoforms of Neurofascin have distinct roles in the assembly of nodes of Ranvier in the central nervous system. J Cell Biol 2008; 181(7): 1169-77.

FIGURES AND FIGURE LEGENDS

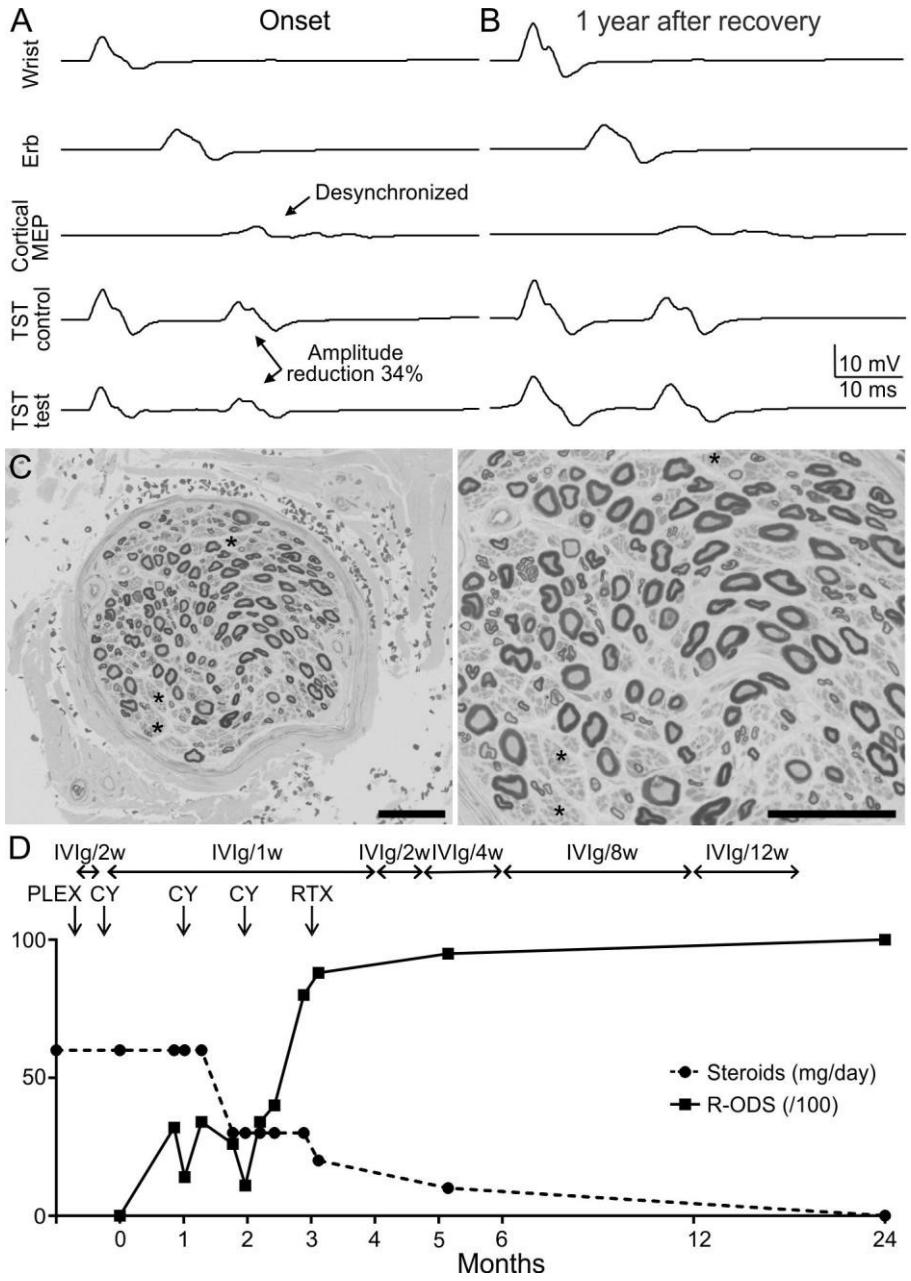

Figure 1: Clinical status of patient CIDP1.

(**A-B**) Conventional transcranial magnetic stimulation with triple stimulation technique (TST) on the left median nerve showed a major desynchronization of the cortical magnetic evoked potential (MEP) and a proximal conduction block when comparing TST control curve and TST test curve amplitude (6.6mV vs 4.4mV, 34% less, normal <10%) at onset (**A**) that both disappeared at one year of follow-up (**B**; 7.9mV vs 8.6mV). The wrist compound muscular amplitude potential increased from 8.2mV at onset to 12.8mV one year after rituximab treatment (+56%). The duration of the cortical MEP decreased from 24.5ms to 18.8ms (30%). (**C**) Transverse sections of sural nerve biopsy stained with paraphenylenediamine. Nerve biopsy

reveals slight axonal loss affecting large and small-diameter fibers, without onion bulb formation or cellular infiltration or immunoglobulin deposits.

(**D**) Evolution of the disabilities measured with the Rasch-Built overall disability scale (RODS) and of the steroid dosage (mg/day) during a two-year follow up. CY = cyclophosphamide ; IVIg = intravenous immunoglobulins ; PLEX = plasma exchange ; RTX = rituximab.

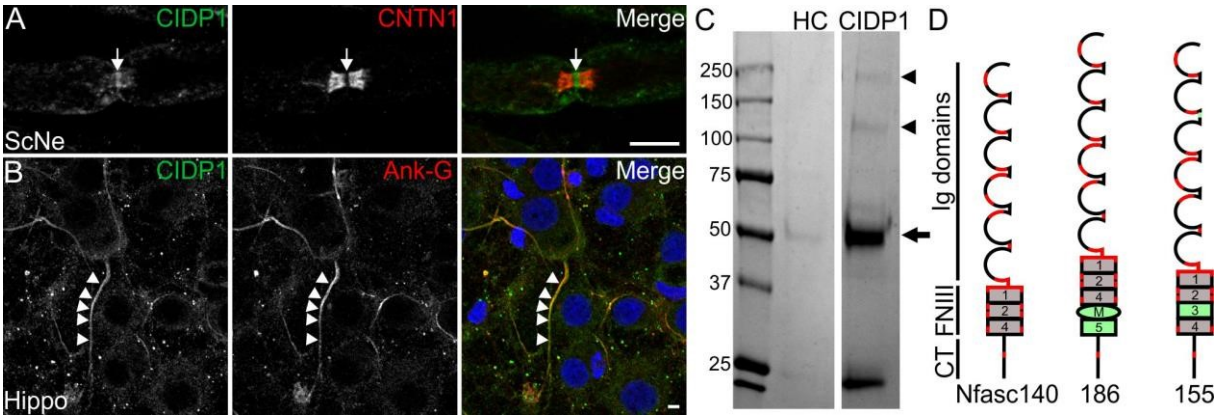

Figure 2: Identification of neurofascin as a nodal target for autoantibodies in CIDP.

(**A**) These are mouse sciatic nerve fibers stained with a CIDP patient's serum (CIDP1; green) and for CNTN1 (red) to label paranodes. Human IgG bound specifically to the node of Ranvier (arrows). (**B**) The patient's IgG (green) bound to surface antigens expressed at the axon initial segment of cultured neocortical neurons (arrowheads), here stained with ankyrin-G (Ank-G; red). Scale bars = 10 µm. (**C**) Neocortical neurons were incubated with sera from a healthy control (HC) or CIDP1 for 1 hour, and the target antigens were immunoprecipitated, separated on SDS-PAGE gels, and stained with imperial blue. Protein bands (arrowheads) were excised and identified by mass spectrometry as neurofascin. Molecular weight markers are shown on the left in kDa. (**D**) Scheme of Nfasc140, 155, and 186 structure showing the position of the immunoglobulin (Ig) and fibronectin type III (FnIII) domains, and of the cytosolic tail (CT). The position of the peptide identified by mass spectrometry is shown in red. The protein sequence difference between neurofascin isoforms is indicated in green.

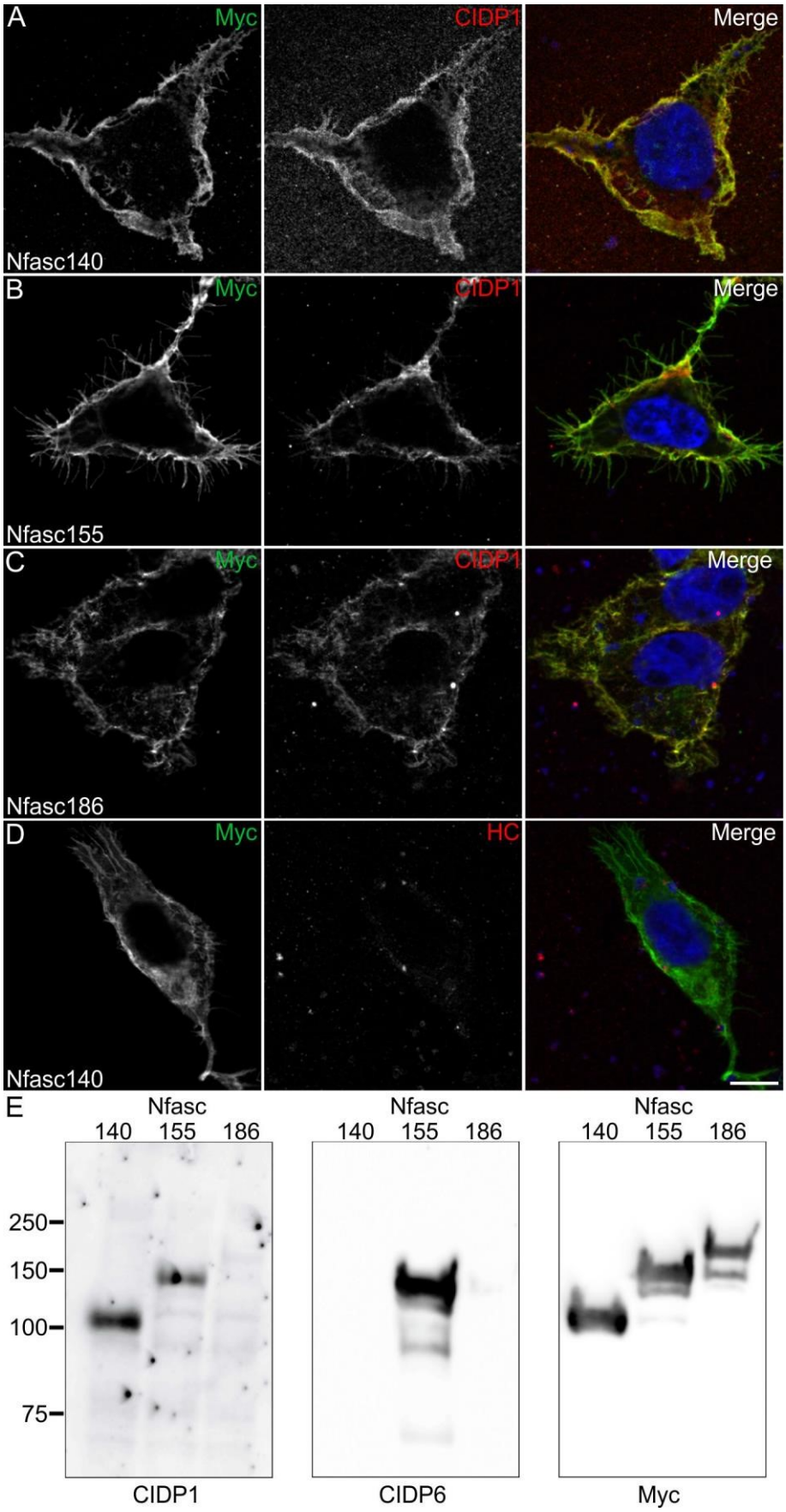

Figure 3: CIDP IgG reacting against nodes recognizes all neurofascin isoforms. (**A-D**) Sera from CIDP1 (**A-C**; red) and from a healthy control (**D**; HC) were tested on living HEK cells transfected with full-length Myc-tagged Nfasc140 (**A** and **D**), Nfasc155 (**B**), and Nfasc186 (**C**).

Neurofascin isoforms were revealed with a monoclonal antibody to Myc (green), and nuclei were stained with DAPI (blue). No healthy control bound to neurofascin isoforms (**D**). The patient's IgG bound more importantly to Nfasc140 and Nfasc186 compared to the Nfasc155. Scale bars = 10 μm. (**E**) Protein samples from Nfasc140, Nfasc155, and Nfasc186 transfected cells were immunoblotted for Myc (right) or with two representative CIDP sera that reacted against nodes (CIDP1) or paranodes only (CIDP6). The mouse anti-Myc antibodies revealed all neurofascin isoforms. The patient CIDP1 reacted against the three Nfasc isoforms, whereas patient CIDP6 only recognized Nfasc155. These results are in keeping with those obtained by ELISA and CBA. Molecular weight markers are shown on the left in kDa.

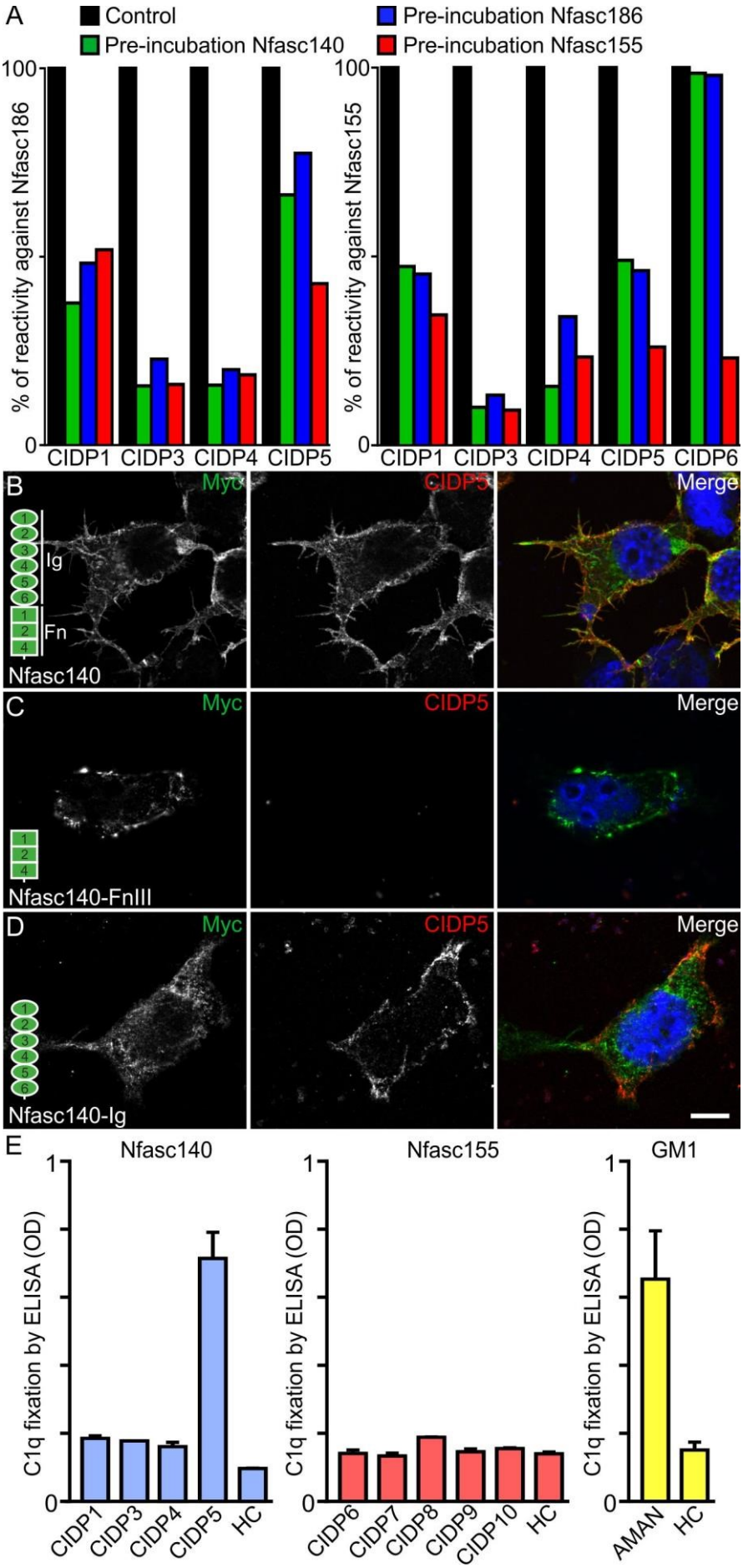

Figure 4: CIDP IgG predominantly recognizes the Nfasc140 isoform.

(**A**) Sera from CIDP patients were pre-incubated with Nfasc140 (green), Nfasc186 (blue), or Nfasc155 (red), then tested by ELISA against Nfasc186 (left) or Nfasc155 (Right). The reactivity after depletion was normalized to that of the CIDP sera prior to depletion (control, black). The pre-incubation with Nfasc140, Nfasc155 or Nfasc186 abolished the reactivity against Nfasc186 and Nfasc155 in most patients with anti-Nfasc140/186 IgG (CIDP1-5). By contrast, solely the pre-incubation with Nfasc155 abolished the reactivity of patients with antiNfasc155 IgG4 (CIDP6). (**B-D)** CIDP sera were tested on living HEK cells transfected with full-length Myc-tagged Nfasc140 (**B)** or with constructs encoding solely the fibronectin type III (FnIII) (**C**) or the immunoglobulin (Ig) domains (**D**). A scheme of Nfasc140 constructs is inserted in each panel. Nfasc140 was revealed with a monoclonal antibody to Myc (green), and nuclei were stained with DAPI (blue). Anti-Nfasc140/186 IgG reacted predominantly against the Ig domains of Nfasc140. Scale bars = 10 μm. (**E**) C1q fixation of patients' antibodies was examined by ELISA. Only one CIDP patient reactive against Nfasc140 (CIDP5) activated complement *in vitro*. No anti-Nfasc155 IgG4 activated complement. As positive control, complement fixation was tested with an acute motor axonal neuropathy sample against GM1. A serum from a healthy control (HC) was used as a negative control in all experiments.

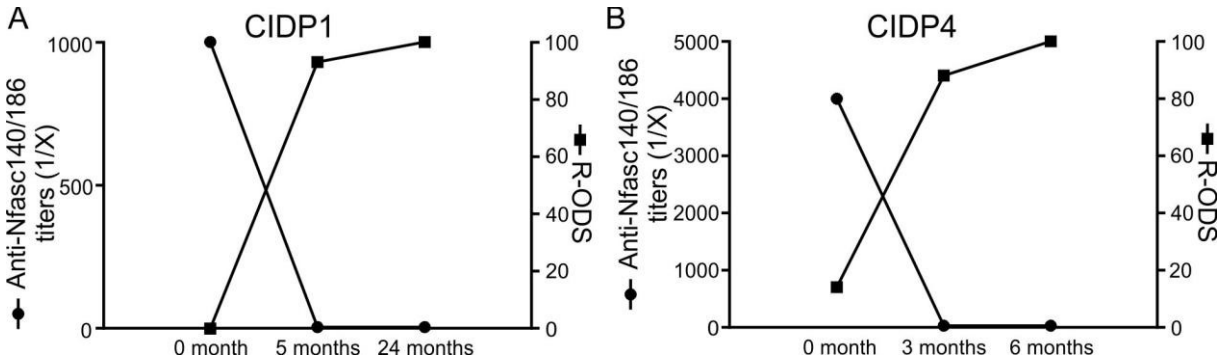

Figure 5: Correlation between anti-Nfasc140/186 IgG titers and the clinical status.

(**A-B**) The evolution of disabilities was measured with the Rasch-Built overall disability scale (R-ODS) in two CIDP patients (CIDP1 and 4). The titers of anti-Nfasc140/186 were measured by ELISA. Clinical remission matched with the depletion of anti-Nfasc140/186 IgG in the two patients.

Table

1: Reactivity of CIDP patients against neurofascin isoforms and nerve tissue.

	IgG titers against			Isotypes	Nerve staining
	Nfasc186	Nfasc140	Nfasc155		
CIDP1	500	1000	1000	IgG4	Node
CIDP2	500	-	-	IgG4>IgG2	Node
CIDP3	1000	2000	2000	IgG4>IgG2	Node
CIDP4	4000	4000	1000	IgG4	Node
CIDP5	6000	6000	7000	IgG3>IgG4	Node
CIDP6	-	-	6000	IgG4	Paranode
CIDP7	-	-	1000	IgG4	Paranode
CIDP8	-	-	6000	IgG4>IgG2	Paranode
CIDP9	-	-	5000	IgG4	Paranode
CIDP10	-	-	3000	IgG4	Paranode

2: Clinical features of patients with anti-Nfasc140/186 IgG.

	CIDP1	CIDP2	CIDP3	CIDP4	CIDP5
Gender	M	F	M	M	F
Age at onset	61	70	2	75	50
Previous infection	Sore throat and bronchitis	Infection	No	No	No
Other dysimmune disease	Anti Ro/SSA	RPF	No	MN	FSGS
Onset	Subacute	Subacute	Subacute	Chronic	Subacute
Sensory ataxia	Yes	Yes	No	Yes	Yes
Neuropathic pain	No	No	No	No	No

Table

Cranial nerve involvement	Yes	No	No	No	Yes
Modified Rankin Scale	5	4	4	4	5
Tremor	No	No	No	No	No
Respiratory failure	Yes	No	No	No	Yes
Intensive care unit	Yes	No	No	No	Yes
Nerve conduction study					
Demyelinating or axonal	Demyel.	Demyel.	Demyel.	Axonal	Axonal
Axonal loss	Yes	Yes	No	No	Yes
Conduction blocks	Yes	Yes	Yes	No	No
Nerve Biopsy	Mild axonal loss	ND	ND	ND	ND
Treatments					
IVIg	Yes	Yes	Yes	ND	No
Plasma exchange	Worsening	ND	ND	ND	Yes
Steroids	Yes	No	No	Yes	Yes
Other effective treatments	CY, RTX	ND	ND	ND	ND

CY = cyclophosphamide; FSGS = focal segmental glomerulosclerosis; IVIg = intravenous immunoglobulins; MN = membranous nephropathy; ND = not done; RPF = retroperitoneal fibrosis; RTX = rituximab.

3: Comparison of clinical features of patients with anti-Nfasc140/186 IgG or antiNfasc155 and of seronegative CIDP patients.

	Anti-Nfasc140/186 IgG	Anti-Nfasc155 IgG4‡	Seronegative
Number	5	74	76
Age in years, median (range)	61 (2-70)	29 (10-76)	58 (22-82)
Sex, male, n (%)	3 (60%)	48 (69%)	30 (39%)
Subacute onset, n (%)	4 (80%)*	13/55 (24%)	4 (5%)
Sensory ataxia, n (%)	4 (80%)	45/70 (64%)*	29 (38%)
Tremor, n (%)	0	31/70 (44%)*	14 (18%)

Table

Cranial nerve involvement, n (%)	2 (40%)	7/32 (22%)	7 (9%)
CNS demyelination, n (%)	0	7/70 (10%)	0
Modified Rankin scale, median (range)	4 (4-5)*	3 (1-5)	2 (0-5)
Good response, n (%)			
IVIg	3/4 (75%)	16/70 (23%)*	48/60 (80%)
Steroids	3/4 (75%)	34/70 (49%)	19/27 (70%)

CNS = central nervous system; IVIg = intravenous immunoglobulin ; ‡ taken from Ng *et al.*, 2012; Querol *et al.*, 2014; Ogata *et al.*, 2015b; Devaux *et al.*, 2016; Kadoya *et al.*, 2016; * $p <$ 0.001 compared to seronegative CIDP patients.

SUPPLEMENTARY TEXT Description of patient CIDP3

The patient is a male child born from non-consanguineous healthy parents with normal delivery and uneventful pregnancy. Psychomotor development was normal until the onset of the disease. No known infectious episodes was seen before the onset of the symptoms.

The first symptoms appeared at 17 months. The patients showed frequent falls and a walking instability. Even though the patient was very young, video provided by the parents indicated that the patient's gait was absolutely normal before the first symptoms. The patient presented normal creatine kinase and hyporeflexia in lower limbs.

Spontaneous improvements for 10 days were seen at three and eight months after the onset with subsequent recurrence of motor deficit.

At 23 months of age when the electrophysiological measurements were performed, the child could stand but not with feet together. He showed waddling and steppage gait for only few steps. He presented Gowers' sign in climbing from the floor, standing up only by external support, and areflexia in lower limbs. Upper limbs had normal strength and normal reflexes. The patient did not show tremor or dysmetria.

Excellent responses to IVIg were observed up to complete recovery, but the patient required regular treatments (every 3-4 weeks). Whenever the treatment was stopped, the patient relapsed. Only motor deficits were seen during these relapses, no additional symptoms or signs.

Supplemental Figure 1: Peptide sequences identified by mass spectrometry.

The amino acid sequences of human Nfasc140 (XM_011509328.1), Nfasc155 (NM_001160331.1), and Nfasc186 (NM_001005388.2) are aligned. Peptide sequences identified by mass spectrometry are highlighted in red.

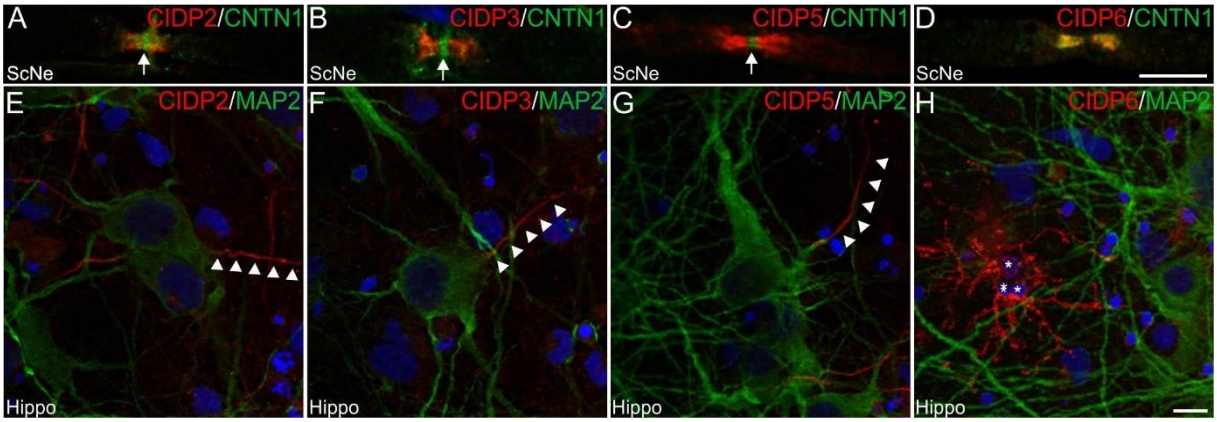

Supplemental Figure 2: Reactivity of CIDP sera against nodes and axon initial segments. These are pictures of four representative CIDP sera tested on teased sciatic nerve fibers (**A-D**) and cultured neocortical neurons (**E-H**) and stained for CNTN1 (green; **A-D**) or microtubuleassociated protein 2 (MAP2; green**; E-H**). Sera from three CIDP patients with antiNfasc140/186 IgG (CIDP2, 3, and 5) stained the nodes (arrows) and axon initial segments (arrowheads). By contrast, the serum from a CIDP patient with anti-Nfasc155 IgG4 (CIDP6) stained only the paranodes (**D**) and reacted against surface epitopes on oligodendrocytes present in the culture (asterisk in **H**). Scale bars = 10 μm.

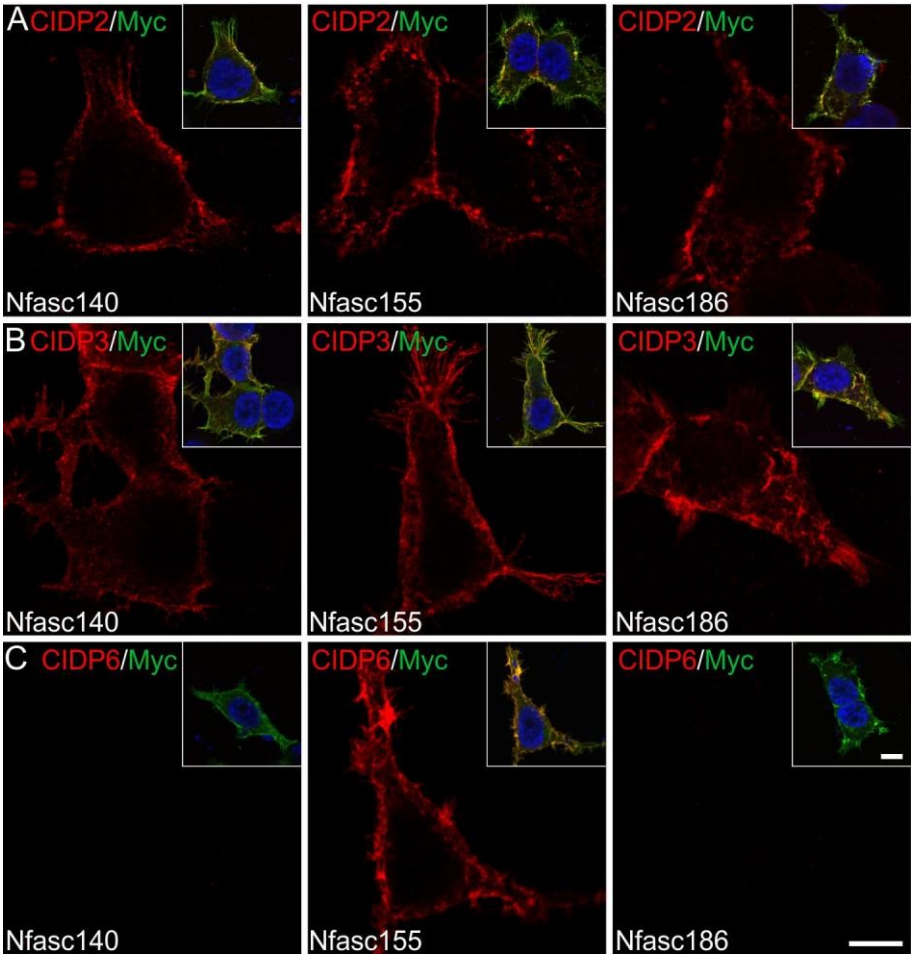

Supplemental figure 3: Reactivity toward neurofascin isoforms of CIDP sera.

These are HEK cells transfected with full-length Myc-tagged Nfasc140, Nfasc155, and Nfasc186 as indicated, and incubated with three representative CIDP sera. The IgG (red) from two CIDP patients (CIDP2 and 3; **A**-**B**) reacted against all three neurofascin isoforms. By contrast, CIDP6 specifically recognized Nfasc155, but did not react against the other isoforms (**C**). Scale bars = 10 μm.

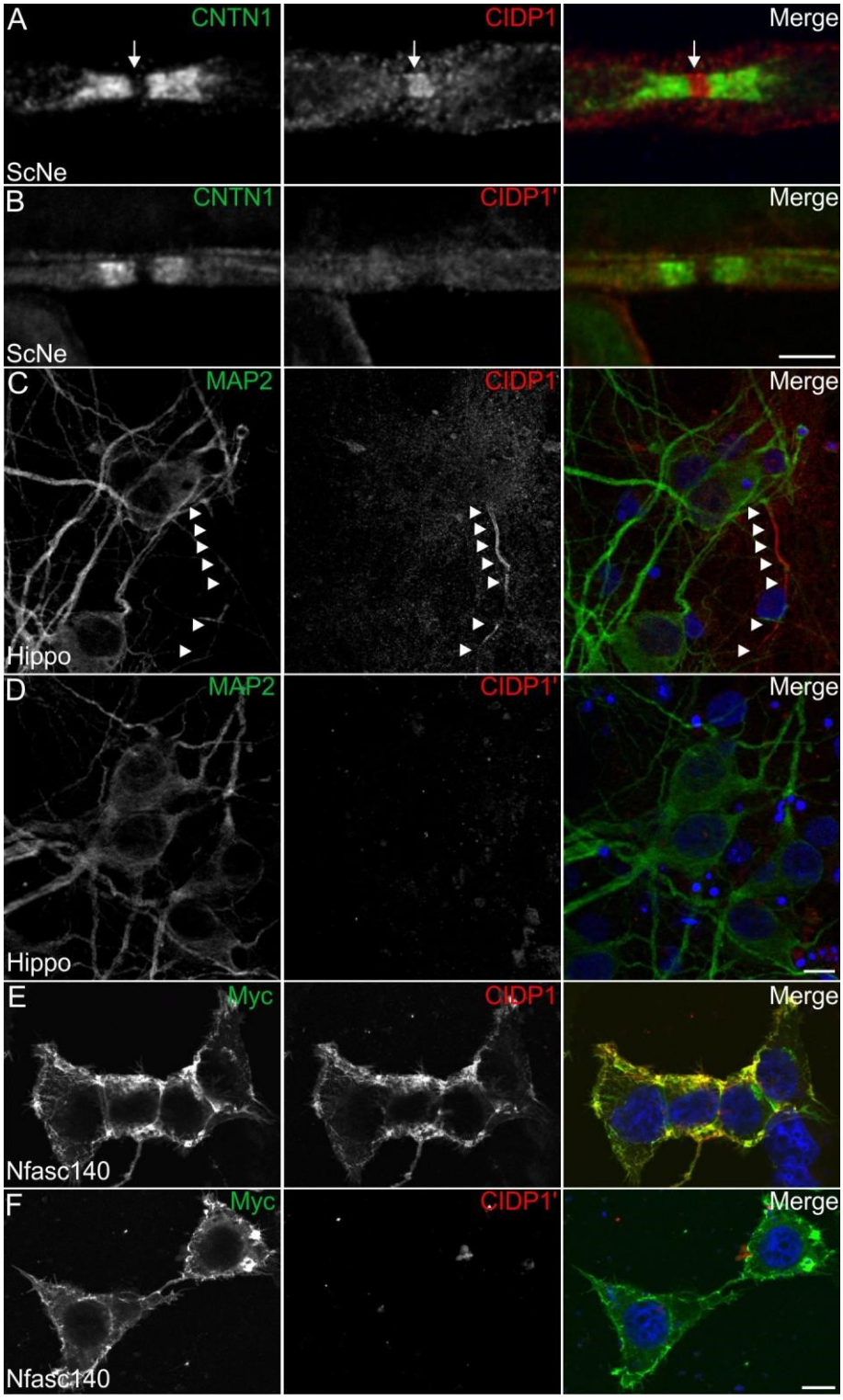

Supplemental Figure 4: The reactivity of CIDP sera against nodes and Nfasc140 is lost after rituximab treatment.

(**A-D**) Teased sciatic nerve fibers (**A-B**) and cultured neocortical neurons (**C**-**D**) were stained with the sera of CIDP1 at onset (red) and one year after rituximab treatment (CIDP1'; red) and for CNTN1 (green; **A-B**) or microtubule-associated protein 2 (MAP2; green**; C**-**D**). The patient's IgG bound to nodes (arrows) and axon initial segment (arrowheads) prior to treatment

but not one year after rituximab treatment. (**E-F**) HEK cells transfected with full-length Myctagged Nfasc140 were stained with the serum of patient CIDP1 at onset (red). Reactivity to Nfasc140 was completely lost after rituximab treatment (CIDP1'; red). Scale bars = 10 μm.